Shaping Multidimensional Signal Spaces—Part I: Optimum Shaping, Shell Mapping

Amir K. Khandani and Peter Kabal

Abstract—In selecting the boundary of a signal constellation used for data transmission, one tries to minimize the average energy of the constellation for a given number of points from a given packing. The reduction in the average energy per two dimensions due to the use of a region $\mathscr{C}$ as the boundary instead of a hypercube is called the shaping gain γ_s of $\mathscr{C}$. The price to be paid for shaping involves: 1) an increase in the factor constellation–expansion ratio (CER$_s$), 2) an increase in the factor peak-to-average-power ratio (PAR), and 3) an increase in the addressing complexity. In general, there exists a tradeoff between γ_s and CER$_s$, PAR. In this work, the structure of the region which simultaneously optimizes both of these tradeoffs is introduced. In an N-D (N-dimensional) optimum shaping region (N even), a 2-D sphere is the boundary of the 2-D subspaces and an N-D sphere is the boundary of the whole space. Analytical expressions are derived for the optimum tradeoff curves. By applying a change of variable denoted as shell mapping, the optimum shaping region is mapped to a hypercube truncated within a simplex. This mapping facilitates the performance computation, and also the addressing of the optimum shaping region. Using shell mapping, we introduce an addressing scheme with low complexity to achieve a point on the optimum tradeoff curves. To obtain more flexibility in selecting the tradeoff point, a second shaping method with more degrees of freedom is used. In this method, a 2-D sphere is the boundary of the 2-D subspaces, an N'-D sphere, $N' \geq 2$, is the boundary of the N'-D subspaces, and an N-D sphere is the boundary of the whole space.

Index Terms—Optimum shaping, shell mapping, truncated cube, uniform density, optimum tradeoff.

I. INTRODUCTION

A 2-D (two-dimensional) signal constellation C_2 is a finite set of 2-D points bounded within a shaping region $\mathscr{C}_2$. In using such a constellation for signaling over a channel, the energy associated with different signal points is not the same. By transmitting the points of higher energy less frequently, one can obtain a lower

average energy for a given entropy [1]. For a fixed number of signal points, such a nonuniform probability distribution reduces the entropy of the set and, consequently, one needs more points to transmit at the same rate. Increasing the number of signal points is a price to be paid for the reduction in the average energy, and is denoted by the factor constellation-expansion ratio (CER$_s$). To expand the constellation, some points of higher energy are added around the existing points. This increases the peak-to-average-power ratio (PAR) of the constellation. The PAR affects the sensitivity of the constellation to nonlinearities and other signal-dependent perturbations.

In using a nonequiprobable signaling scheme with a signal constellation C_2, as the rate transmitted per channel use is not constant, we can have a variable delay in transmission. A method to avoid this problem based on using a shaping code (which has a fixed rate per signaling interval) is given in [1]. Another approach is to use an N-D signal constellation C_N ($N > 2$) which is selected as an appropriate subset of the $N/2$-fold Cartesian product of C_2 with itself. This subset is selected by a region $\mathscr{R}_N$. The final shaping region is denoted as $\mathscr{C}_N$, i.e., $\mathscr{C}_N = \mathscr{R}_N \cap \{\mathscr{C}_2\}^{N/2}$ where $\mathscr{C}_2$ is the shaping region associated with C_2 and $\{\mathscr{C}_2\}^{N/2}$ is its $N/2$-fold Cartesian product. In this case, using the points of C_N with equal probability induces a nonuniform probability distribution on the points of C_2. This is the basic idea of constellation shaping.

Addressing is the assignment of the data bits to the constellation points. If $C_N = \{C_2\}^{N/2}$, the addressing in C_N can be achieved independently along each C_2. For a shaped constellation, which is a subset of $\{C_2\}^{N/2}$, independent addressing is not applicable, and we need a means to specify that certain elements of $\{C_2\}^{N/2}$ are not allowed. This means that the use of shaping increases the addressing complexity. For a fixed number of bits per dimension, a multidimensional constellation can have a huge number of points. This can make the addressing of such a constellation a complicated problem.

In the work of Wei [2], shaping is a side effect of the method employed to transmit a nonintegral number of bits per two dimensions. This method provides moderate shaping gain for low values of CER$_s$. Addressing of this shaping method is achieved by a lookup table. Forney and Wei generalize this method under the topic of the generalized cross constellations in [3]. They also find the opti-

mum induced probability distribution on the 2-D sub-spaces (for an infinite dimensional space) and calculate the corresponding tradeoff curves.

Conway and Sloane in [4] introduced the idea of the Voronoi constellation based on using the Voronoi region of a lattice Λ_s as the shaping region. The Voronoi constellations are further considered and elaborated on by Forney in [5].

In [1], Calderbank and Ozarow introduced a shaping method which is directly achieved on the 2-D subspaces. In this method, the 2-D subspaces are partitioned into equal volume circular subregions of increasing average energy. A shaping code is then used to specify the sequence of subregions. The shaping code is designed so that the lower energy subregions are used more frequently. As all the codewords of the shaping code are equiprobable, the total rate per signaling interval remains constant. They also find the optimum induced probability distribution on the 2-D subregions (for an infinite dimensional space) and calculate the corresponding tradeoff curves.

Lang and Longstaff in [6] use an addressing scheme to address the points of a spherical constellation based on the Leech lattice. In their scheme, first, the final constellation is divided into energy shells. Then, a point in a shell is found by successively decomposing the space into lower dimensional subspaces via generating function techniques. The key point to this scheme is that the energy along different dimensions has an additive property. Prior to [6], a similar addressing scheme was used by Fischer in [7] to label the points of a vector quantizer with a pyramidal quantization region.

The idea of trellis shaping is introduced in [8]. This is based on using an infinite-dimensional Voronoi region determined by a convolutional code to shape the constellation.

In [9], Kschischang and Pasupathy discuss a shaping method which is based on using the 2-D points with nonequal probability. In [10], Livingston discusses a shaping method in which the 2-D subspaces are partitioned into circular shells of increasing size. In this method, the 2-D shells are used with equal probability inducing a nonuniform distribution on the 2-D points.

In a continuation to [1] and [10], Calderbank and Klimesh in [11] use a balanced binary code to select the sequence of the 2-D circular shells. In their scheme, as all the shaping codewords have an equal number of zeros and ones, independent of the size of the circular shells, the data rate per signaling interval remains constant.

In this work, we study two methods for shaping. In the first method, a 2-D sphere is the boundary of the 2-D subspaces and an N-D sphere is the boundary of the whole space. The final region, which is denoted as $\mathscr{A}_N$, results in the optimum tradeoff between γ_s and CER_s, and also between γ_s and PAR. In this case, the ratio of the radii of the two spheres determines the corresponding tradeoff point. Analytical expressions are derived for the tradeoff as a function of dimensionality. We describe a

method to achieve a point with low addressing complexity on the optimum tradeoff curves. To obtain more flexibility in selecting the tradeoff point, a second shaping method with two degrees of freedom is used. In this method, an $\mathscr{A}_{N'}$ region is employed along the N'-D subspaces, and then the Cartesian product $\{\mathscr{A}_{N'}\}^{n'}$, $n' = N/N'$ is further shaped by the use of an N-D sphere.

In all our discussions, we assume that the dimensionality is even and the constellation points are used with equal probability.

II. DEFINITIONS

By selecting the region $\mathscr{C}_N$ as the boundary of a constellation (instead of a hypercube), the average energy per two dimensions P_2 reduces by the factor [3]

$$\gamma_s(\mathscr{C}_N) = \frac{[V(\mathscr{C}_N)]^{2/N}}{6P_2(\mathscr{C}_N)} \qquad (1)$$

where $V(\mathscr{C}_N)$ is the volume of $\mathscr{C}_N$. This is called the shaping gain of $\mathscr{C}_N$.

For a given integer l, assume that the space dimensions are indexed by $i = lp + m$, where $p = 0, \cdots, (N/l) - 1$ and $m = 0, \cdots, l - 1$. The subspaces spanned by the set of vectors with the same index p are called the constituent l-D subspaces [3]. The region $\mathscr{C}_N$ is called l-dimensional symmetric if its projection on all the constituent l-D subspaces is the same [3]. In the present work, all the discussions are based, as is conventional, on two-dimensional symmetric regions. The more general case of the l-dimensional symmetric regions is discussed in [12]. A two-dimensional symmetric region can be written as $\mathscr{C}_N = \mathscr{R}_N \cap \{\mathscr{C}_2\}^{N/2}$ where $\mathscr{C}_2$ is the projection of $\mathscr{C}_N$ on the constituent 2-D subspaces.

The constellation-expansion ratio (CER_s) is the ratio of the volume per two dimensions to the minimum necessary volume per two dimensions [3], i.e.,

$$\text{CER}_s(\mathscr{C}_N) = \frac{V(\mathscr{C}_2)}{[V(\mathscr{C}_N)]^{2/N}}. \qquad (2)$$

As an alternative to CER_s, we define the shaping redundancy in bits per N dimensions as

$$r_s(\mathscr{C}_N) = (N/2)\log_2(\text{CER}_s). \qquad (3)$$

Let $E_P(\mathscr{C}_2)$ denote the peak energy of $\mathscr{C}_2$. The peak-to-average-power ratio (PAR) is defined as [3]

$$\text{PAR}(\mathscr{C}_N) = \frac{E_P(\mathscr{C}_2)}{P_2(\mathscr{C}_N)}. \qquad (4)$$

In general, there exists a tradeoff between γ_s and CER_s (or r_s), and also between γ_s and PAR. In the following, the structure of the region which optimizes both of these tradeoffs is introduced. This region has the minimum second moment (energy) for a given volume and given CER_s or for a given volume and given PAR.

III. OPTIMUM SHAPING REGION

In an optimally shaped region, a 2-D sphere of radius R_2, $\mathscr{S}_2(R_2)$ is the boundary of the 2-D subspaces and an N-D sphere of radius R_N, $\mathscr{S}_N(R_N)$ is the boundary of the whole space. The final region is denoted as $\mathscr{A}_N$, i.e.,

$$\mathscr{A}_N = \{X_i, i = 0, \cdots, N - 1\}$$
$$: 0 \leq X_{2p}^2 + X_{2p+1}^2 \leq R_2^2,$$
$$p = 0, \cdots, n - 1, n = N/2,$$
$$0 \leq \sum_{i=0}^{N-1} X_i^2 \leq R_N^2, \qquad 0 \leq R_N^2 \leq nR_2^2. \quad (5)$$

We say that the shaping of $\mathscr{A}_N$ is achieved in two steps. The first step is by the use of $\mathscr{S}_2$'s and the second step is by the use of $\mathscr{S}_N$. In general, the projection of the region $\mathscr{A}_N$ on any of its constituent l-D subspaces, l being an even integer greater than two, is the region $\mathscr{A}_l$ with the same values for the radii of the shaping spheres as the original $\mathscr{A}_N$ region. This results in a recursive structure. In the following, we first prove that the $\mathscr{A}_N$ region results in the optimum tradeoff between CER_s and γ_s. Then, we prove the optimality of the tradeoff between PAR and γ_s.

Consider a two-dimensional symmetric region $\mathscr{C}_N = \mathscr{R}_N \cap \{\mathscr{C}_2\}^{N/2}$. For a given $V(\mathscr{C}_N)$ and CER_s, we would like to maximize γ_s. From (1), this is equivalent to minimizing $P_2(\mathscr{C}_N)$. From (2), $V(\mathscr{C}_N)$ and CER_s being fixed implies that $V(\mathscr{C}_2)$ is fixed. With these quantities fixed, CER_s does not depend on the shape of the regions $\mathscr{R}_N$ and $\mathscr{C}_2$. For a given $\mathscr{C}_2$, the region $\mathscr{R}_N$ should select a subset of $\{\mathscr{C}_2\}^{N/2}$ which has the minimum second moment for a given volume. This implies that $\mathscr{R}_N$ is an N-D sphere. Similarly, for a given $\mathscr{R}_N$, the region $\{\mathscr{C}_2\}^{N/2}$ should select a subset of $\mathscr{R}_N$ which has the minimum second moment for a given volume. This implies that $\mathscr{C}_2$ is a circle.

Furthermore, it can be shown [3] that

$$\mathrm{PAR}(\mathscr{C}_N) = \frac{\mathrm{PAR}(\mathscr{C}_2)}{\gamma_s(\mathscr{C}_2)} \times \gamma_s(\mathscr{C}_N) \times \mathrm{CER}_s(\mathscr{C}_N). \quad (6)$$

But, a sphere is the 2-D figure which maximizes $\gamma_s(\mathscr{C}_2)$ and minimizes the $\mathrm{PAR}(\mathscr{C}_2)$. Using these facts, and also the optimality of the tradeoff between γ_s and CER_s in (6), proves the optimality of the tradeoff between γ_s and PAR.

In the following, the technique of shell mapping is introduced. This is a change of variable which maps the optimum shaping region to a hypercube truncated within a simplex. This mapping has some nice properties which facilitate the performance computation, and also the addressing of the optimum shaping region.

IV. SHAPING USING ONE LEVEL OF SHELL MAPPING

By applying the change of variable

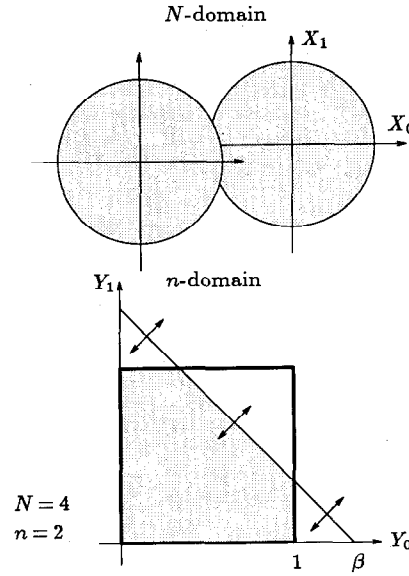$$Y_p = \left(X_{2p}^2 + X_{2p+1}^2\right)/R_2^2, \qquad p = 0, \cdots, n - 1, n = N/2 \quad (7)$$

Fig. 1. Example of the $\mathscr{A}_4$ region, one-level shell mapping. Each 2-D subspace in the 4-D space is mapped to one of the axes of the $\mathscr{T}\mathscr{C}_2$.

to (5), the $\mathscr{A}_N$ region is mapped to the following n-D solid:

$$\mathscr{T}\mathscr{C}_n(1, \beta) = \{Y_p, p = 0, \cdots, n - 1\}$$
$$: 0 \leq Y_p \leq 1,$$
$$0 \leq \sum_{p=0}^{n-1} Y_p \leq \beta,$$
$$0 \leq \beta = R_N^2/R_2^2 \leq n. \quad (8)$$

This is a hypercube of edge length one truncated within a simplex of edge length β. We refer to the N-D space as the N-domain and to the n-D space as the n-domain. This mapping, which is denoted as the shell mapping, is the key point to most of our discussions. Fig. 1 shows an example for $N = 4$.

Shell mapping has the following properties.

• A uniform density of points within $\mathscr{A}_N$ results in a uniform density of points within $\mathscr{T}\mathscr{C}_n$. This fact can be developed considering that for a uniform density in a spherically symmetrical region in 2-D (a circle in our case), the transformation from the rectangular coordinates (X_0, X_1) to the spherical coordinates $(U = X_0^2 + X_1^2, \Theta)$ gives a uniform U. This property allows us to achieve the shaping and the addressing on equal volume partitions of $\mathscr{T}\mathscr{C}_n$.

• Unlike the $\mathscr{A}_N$ region, the boundaries of $\mathscr{T}\mathscr{C}_n$ are hyperplanes. This makes the partitioning and the addressing of $\mathscr{T}\mathscr{C}_n$ an easier task than that of $\mathscr{A}_N$.

• For $\beta = n/2$, the simplex in (8) divides the hypercube into two congruent partitions, each of volume $1/2$. The $\mathscr{T}\mathscr{C}_n$ region is equal to one of them. This is equal to the Voronoi region of the lattice D_n^* [13] in the positive coordinates. This allows us to use a Voronoi constellation [5] for the addressing.

• The project of the region $\mathcal{TC}_n(1, \beta)$ on any of its l-D subspaces is the region $\mathcal{TC}_l(1, \beta)$. This provides a strong framework for a recursive addressing structure. This property is the basis for the addressing schemes of [14], [15].

These properties are extensively used in the companion paper [15] to facilitate the addressing.

V. SHAPE GAIN TRADEOFF

In the Appendix, the integral of a function of the general form $F(X_0^2 + \cdots + X_{N-1}^2)$ over the $\mathcal{A}_N$ region is calculated as

$$\int_{\mathcal{A}_N} F(X_0^2 + \cdots + X_{N-1}^2)\, dX_0 \cdots dX_{N-1}$$

$$= (\pi R_2^2)^n \sum_{k=0}^{\lfloor \beta \rfloor} (-1)^k C_n^k \frac{(\beta - k)^n}{(n-1)!}$$

$$\cdot \int_0^1 F\{R_2^2[(\beta - k)\tau + k]\}\tau^{n-1}\, d\tau. \quad (9)$$

This integral is used to calculate the volume and the second moment of the $\mathcal{A}_N$ region. The results, together with $V(\mathcal{C}_2) = \pi R_2^2$ and $E_P(\mathcal{C}_2) = R_2^2$, are used in (1), (2), and (4) to compute γ_s, CER_s, and PAR. Fig. 2 shows the corresponding tradeoff curves for different values of N. The curves corresponding to $N = \infty$ are extracted from [3]. In [12], it is proved that as $N \to \infty$, the induced probability distribution along 2-D subspaces of the $\mathcal{A}_N$ region tends to a truncated Gaussian distribution. This justifies the use of the curves obtained in [3] for the $\mathcal{A}_\infty$ region. Obviously, this is a consequence of the optimality of these regions.

We use $\psi = \beta/n$ $(n = N/2)$ as the normalized parameter for the $\mathcal{A}_N$ region. The complete notation for the region is $\mathcal{A}_N(\psi)$. For $\psi = 1/n$ $(\beta = 1, R_N = R_2)$, we obtain the spherical region $\mathcal{S}_N(R_N)$. This case corresponds to the final point on the tradeoff curves. For $1/n < \psi < 1$ $(1 < \beta < n, R_2 < R_N < \sqrt{n}\, R_2)$, by increasing ψ, we move along the curves towards their initial parts. Finally, for $\psi = 1$ $(\beta = n, R_N = \sqrt{n}\, R_2)$, we have $\mathcal{A}_N = \{\mathcal{S}_2(R_2)\}^n$. This results in the starting point on the tradeoff curves. The two cases of $0 < \psi < 1/n$ and $\psi > 1$ result in the regions $\mathcal{S}_N(\sqrt{n\psi}\, R_2)$ and $\{\mathcal{S}_2(R_2)\}^n$, respectively.

Referring to Fig. 2, it is seen that, in general, the initial parts of the optimum tradeoff curves have a steep slope. This means that an appreciable portion of the maximum shaping gain, corresponding to a spherical region, can be achieved with a small value of CER_s, PAR. Table I contains a set of points from the optimum tradeoff curves. These are the points marked on the curves in Fig. 2. The S-points correspond to a spherical region and achieve the maximum shaping gain in a given dimensionality. The K-points correspond to $r_s = N/4$ $(\text{CER}_s = (2)^{1/2} = 1.41)$. They achieve almost all of the shaping gain of the S-points, but with a much lower value of CER_s, PAR. The L-points correspond to $r_s = N/8$ $(\text{CER}_s = (2)^{1/4} = 1.19)$. They achieve a significant γ_s with a very low CER_s, PAR. The

B-points correspond to $r_s = 3$ $(\text{CER}_s = (8)^{2/N})$. We will return to the B-points later. The A-points correspond to the addressing scheme based on the lattice D_n^*. They result in $r_s = 1$ $(\text{CER}_s = (2)^{2/N})$. For $N = 4$, this point corresponds to a spherical region.

From Fig. 2, it is seen that for N around 12, the A-points with $r_s = 1$ are located near the knee of the optimum tradeoff curves. For larger dimensionalities, specifically for $N > 16$, they are closer to the initial parts of the curves. This means that for $N > 16$, one bit of redundancy per N dimensions is too small. A solution in a space of dimensionality $N = n' \times N'$ (N' even) is to use the lattice D_n^*, $n = N'/2$ to shape the N'-D subspaces and then achieve another level of shaping on the $n' = N/N'$-fold Cartesian product of these subspaces. This is one example of the application of a multilevel shaping/addressing scheme.

More generally, consider an $\mathcal{A}_N(\psi)$ region. This region has an $\mathcal{A}_{N'}(N\psi/N')$ region along each of its constituent N'-D (N' even) subspaces. The basic idea is that we can modify the $\mathcal{A}_{N'}(N\psi/N')$ subregions such that the complexity of the addressing in the N-D space is decreased while the overall suboptimality is small. Specifically, in some of our schemes, 1) the $\mathcal{A}_{N'}(N\psi/N')$ region is replaced by the region $\mathcal{A}_{N'}(1/2)$, and/or 2) this region is partitioned into a finite number of energy shells, and then the Cartesian product of the N'-D subspaces is shaped by a lookup table. These are the bases for the multilevel shell addressed constellations and the addressing decomposition schemes proposed in [15].

In the following, this idea is explained by the use of a more general approach.

VI. SHAPING USING TWO LEVELS OF SHELL MAPPING

In the two-level shell mapping method, shaping is achieved in three steps. In the first two steps, by using the one-level shell mapping method, an $\mathcal{A}_{N'}$ region is employed along the N'-D (N' even) subspaces. In the third step, from the $n' = N/N'$-fold Cartesian product of the $\mathcal{A}_{N'}$ with itself, a subset with a given volume and least second moment is selected. As before, such a subset is selected by a sphere. This results in two degrees of freedom in selecting the final region. This region is denoted as $\mathcal{A}_N^{N'}$, and we have

$$\mathcal{A}_N^{N'} = \{\mathcal{A}_{N'}\}^{n'} \cap \mathcal{S}_N(R_N)$$

$$= \{\mathcal{S}_2(R_2)\}^{nn'} \cap \{\mathcal{S}_{N'}(R_{N'})\}^{n'} \cap \mathcal{S}_N(R_N),$$

$$n' = N/N', n = N'/2. \quad (10)$$

In the case that $\mathcal{A}_{N'}$ is selected as $\{\mathcal{S}_2(R_2)\}^n$, this method reduces to one level of shell mapping.

Assume that the space dimensions are indexed by $i = N'q + 2p + m$ where $q = 0, \cdots, n' - 1$, $p = 0, \cdots, n - 1$, and $m = 0, 1$. Using the change of variable

$$Z_q = \sum_{p=0}^{n-1} \left[X_{2(nq+p)}^2 + X_{2(nq+p)+1}^2 \right] / R_2^2,$$

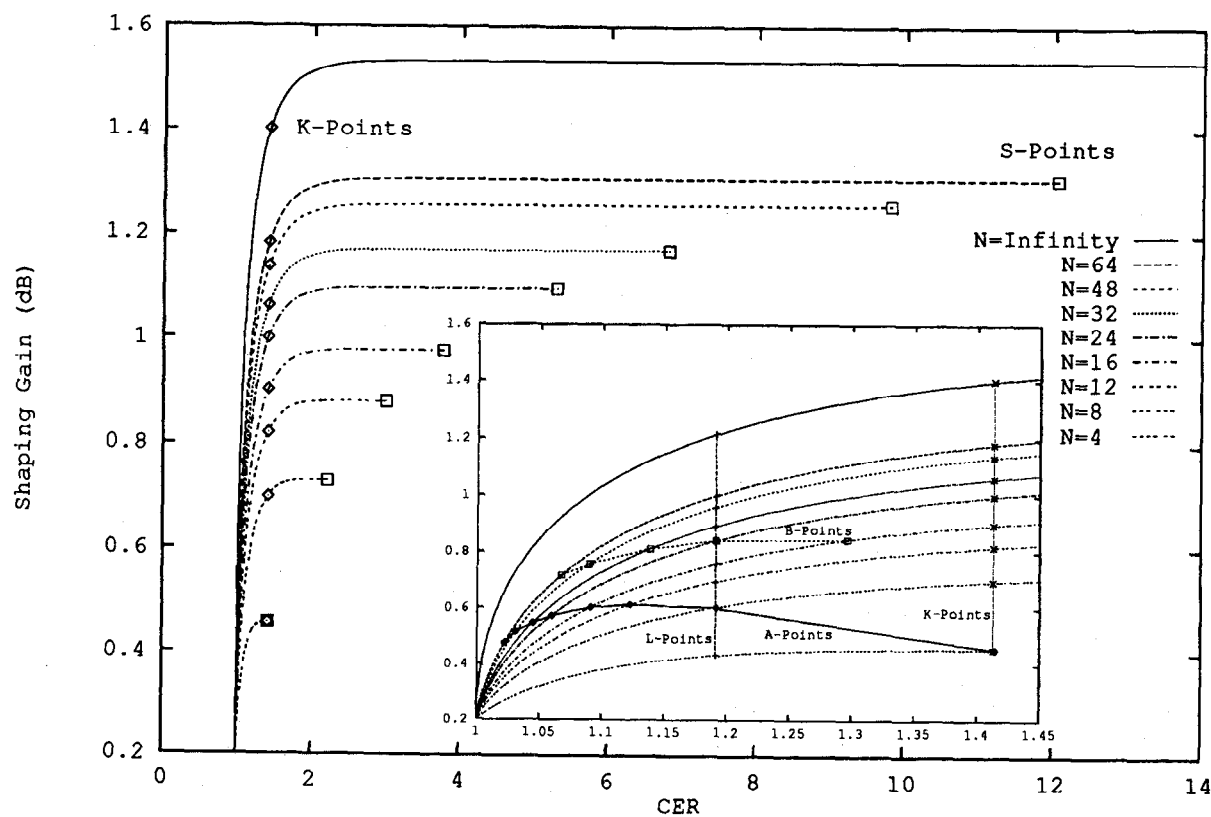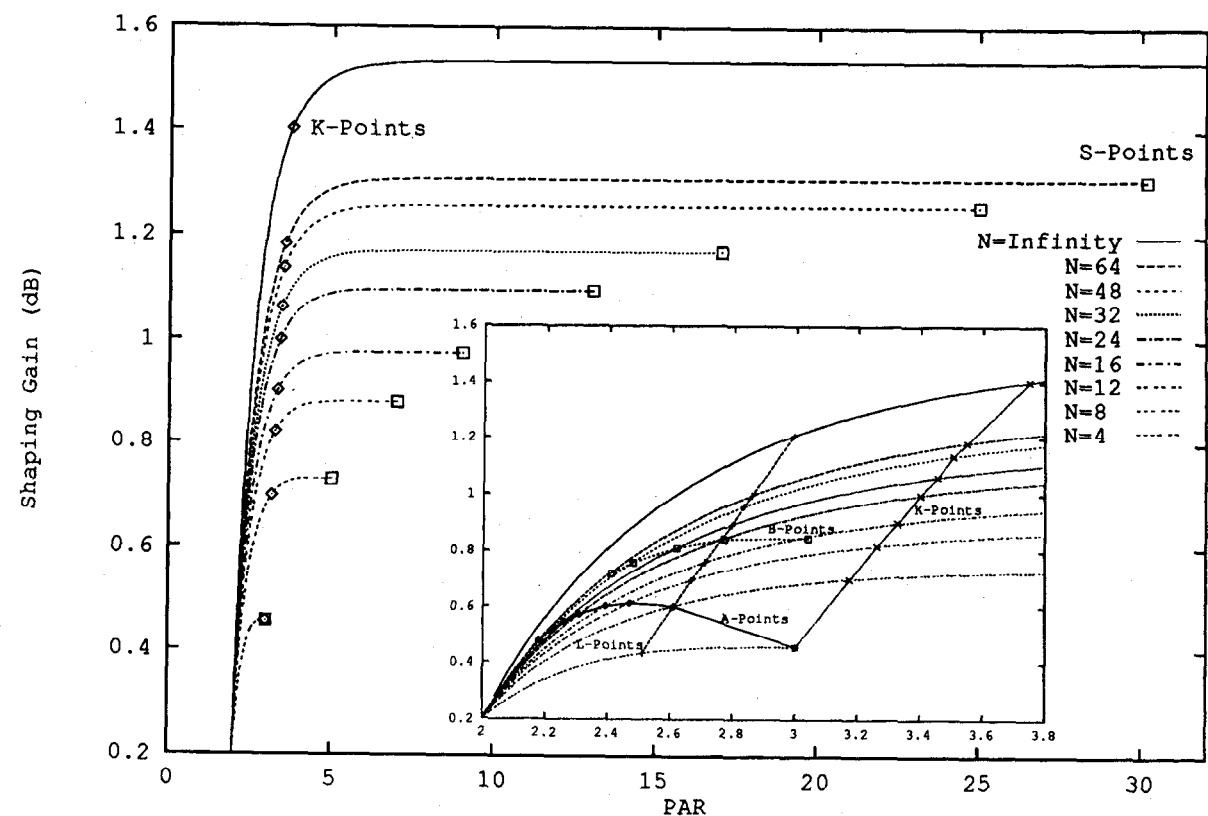$$q = 0, \cdots, n' - 1, p = 0, \cdots, n - 1 \quad (11)$$

Fig. 2.   Tradeoff between γ_s and CER_s, PAR in $\mathscr{A}_N$ region (optimum tradeoff).

TABLE I
A SET OF IMPORTANT POINTS FROM THE OPTIMUM TRADEOFF CURVES

| | A | | | B | | | L | | | K | | | S | | |
N	CER_s	PAR	γ_s dB	CER_s	PAR	γ_s dB	CER_s	PAR	γ_s dB	CER_s	PAR	γ_s dB	CER_s	PAR	γ_s dB
4	1.41	3.00	0.46	—	—	—	—	—	—	1.41	3.00	0.46	1.41	3.0	0.46
8	1.19	2.60	0.60	1.68	3.76	0.72	1.19	2.60	0.60	1.41	3.19	0.70	2.21	5.0	0.73
12	1.12	2.47	0.61	1.41	3.26	0.82	1.19	2.68	0.70	1.41	3.26	0.82	2.99	7.0	0.88
16	1.09	2.39	0.60	1.30	3.04	0.85	1.19	2.71	0.76	1.41	3.33	0.90	3.76	9.0	0.98
24	1.06	2.31	0.57	1.19	2.76	0.84	1.19	2.76	0.84	1.41	3.42	1.00	5.29	13.0	1.10
32	1.04	2.26	0.55	1.14	2.62	0.81	1.19	2.80	0.89	1.41	3.45	1.06	6.80	17.0	1.17
48	1.03	2.22	0.52	1.09	2.48	0.76	1.19	2.83	0.96	1.41	3.51	1.14	9.80	25.0	1.26
64	1.02	2.18	0.48	1.07	2.41	0.72	1.19	2.86	1.00	1.41	3.53	1.18	12.04	33.0	1.31
128	1.01	2.12	0.41	1.03	2.27	0.61	1.19	2.93	1.08	1.41	3.65	1.27	24.67	65.0	1.40
∞	1.00	2.00	0.20	1.00	2.00	0.20	1.19	3.00	1.20	1.41	3.75	1.40	∞	∞	1.53

and defining β and β' by

$$R_{N'}^2 = \beta R_2^2, \quad R_N^2 = \beta\beta' R_2^2, \qquad (12)$$

the region $\mathscr{A}_N^{N'}$ reduces to

$$\mathscr{TC}_{n'}(\beta, \beta\beta') = \{Z_q, q = 0, \cdots, n' - 1\}$$

$$: 0 \le Z_q \le \beta$$

$$0 \le \sum_{q=0}^{n'-1} Z_q \le \beta\beta'. \qquad (13)$$

This is an n'-D simplex of edge length $\beta\beta'$ truncated within a hypercube of edge length β. The n'-D space is denoted as the n'-domain.

The normalized parameters are selected as $\psi = \beta/n$ and $\psi' = \beta'/n'$. The complete notation for the region is $\mathscr{A}_N^{N'}(\psi, \psi')$. For $\psi' = 1$, we have $\mathscr{A}_N^{N'}(\psi, 1) = \{\mathscr{A}_{N'}(\psi)\}^{n'}$. In this case, γ_s, CER_s, and PAR are equal to their corresponding values in $\mathscr{A}_{N'}(\psi)$.

Consider the region $\mathscr{A}_N^{N'}(1/2, \psi')$. This region has an $A_{N'}(1/2)$ region along the N'-D subspaces.[1] In [12], the integral of a function of the general form $F(X_0^2 + \cdots + X_{N-1}^2)$ over the region $\mathscr{A}_N^{N'}$ is calculated. This integral is used to calculate the tradeoff in the $\mathscr{A}_N^{N'}(1/2, \psi')$ region. The result of these calculations for $N = 16, 32$ is shown in Fig. 3. The starting point of the curves ($\psi' = 1$) corresponds to the region $\mathscr{A}_{N'}(1/2)$. It is seen that for relatively high CER_s and for $n' = 2$ ($N' = N/2$), the curves are very near the optimum tradeoff curves.

In practice, we partition each $\mathscr{A}_{N'}(1/2)$ region into K energy shells of equal volume, and select a subset in their n'-fold Cartesian product. These partitions correspond to equal volume partitions in the n-domain produced by the radial hyperplanes, and are denoted by a set of the points $\{U_i, i = 0, \cdots, K\}$ along each dimension of the n'-domain. Then, a subset of the elements in the Cartesian product of the partitions is selected. An example for $N = 8$, $N' = 4$, and $K = 4$ is shown in Fig. 4.

A point U_i on a dimension of the n'-domain corresponds to the region $\mathscr{A}_{N'}$ with $\beta = U_i$. Using (9), the

[1] The corresponding shaping region in the n-domain is the Voronoi region of the lattice D_n^* in the positive coordinates. This is a useful property, and is used in [15] to partition the N'-D subspaces by the use of a lattice partition chain.
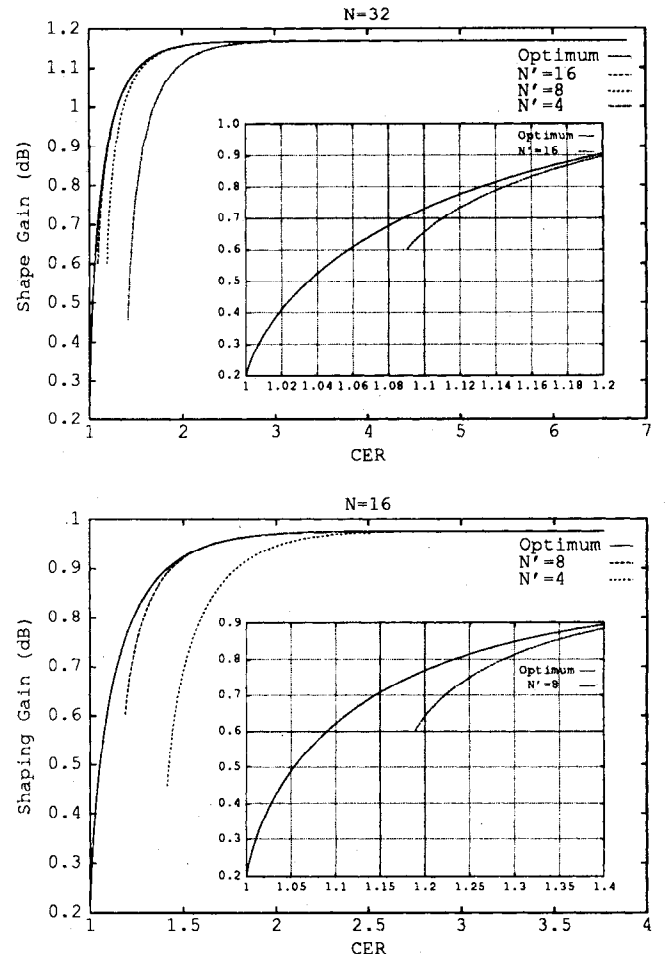

Fig. 3.   Tradeoff between CER_s and γ_s in $\mathscr{A}_N^{N'}(1/2, \psi')$ region, $N = 16, 32$.

volume of this region is equal to

$$V(\mathscr{A}_{N'}(n/U_i)) = (\pi R_2^2)^n \sum_{k=0}^{\lfloor U_i \rfloor} (-1)^k C_n^k \frac{(U_i - k)^n}{n!}. \qquad (14)$$

To obtain partitions of equal volume, the points U_i should satisfy

$$\sum_{k=0}^{\lfloor U_i \rfloor} (-1)^k C_n^k \frac{(U_i - k)^n}{n!} = \frac{i}{K} \sum_{k=0}^{n/2} (-1)^k C_n^k \frac{[(n/2) - k]^n}{n!}. \qquad (15)$$
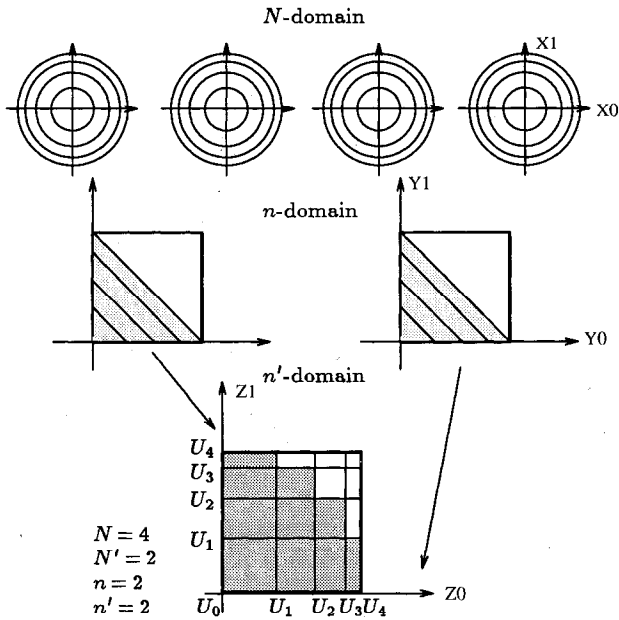
N-domain

n-domain

n'-domain

$N = 4$
$N' = 2$
$n = 2$
$n' = 2$

Fig. 4. Example of the two-level shell mapping.

The summation on the right-hand side is the volume of the region $\mathscr{TC}_n(1, n/2)$ which is equal to $1/2$. Substituting this value in (15), we obtain

$$\sum_{k=0}^{\lfloor U_i \rfloor} (-1)^k C_n^k \frac{(U_i - k)^n}{n!} = \frac{i}{2K}, \qquad i = 1, \cdots, K. \quad (16)$$

Equations (16) can be used to calculate the points U_i (for example, by using a bisection algorithm). The partitioning of the N'-D subspaces results in $K^{n'}$ equal volume partitions in the N-domain. Each of these partitions corresponds to a parallelepiped in the n'-domain. A parallelepiped located at point $(U_{I_0}, \cdots, U_{I_{n'-1}})$, $I_{j \in \{0, \cdots, n'-1\}} \in \{0, \cdots, K\}$ is shown by

$$\mathscr{P}(U_{I_0}, \cdots, U_{I_{n'-1}}) = \{Z_q, q = 0, \cdots, n' - 1\}$$

$$: U_{I_0} \le Z_0 \le U_{I_0 + 1},$$

$$\cdots$$

$$U_{I_{n'-1}} \le Z_{n'-1} \le U_{I_{n'-1} + 1}. \quad (17)$$

Shaping is achieved by selecting T of the N-D partitions with the least second moment. In the example of Fig. 4, we have $T = 10$. Considering that the second moment of the N-domain is proportional to the first moment of the n-domain, the selected subset should correspond to the parallelepipeds with the least average first moment. This procedure, in fact, uses a quantized version of $\mathscr{TC}_{n'}$, denoted as $\mathscr{QTC}_{n'}$, as the shaping region in the n'-domain. The final region is denoted as $\mathscr{QA}_N^{N'}(K, T)$.

In a parallelepiped, the average first moment is equal to the sum of the average first moments along different dimensions. Using this fact, it can be shown that

$$F_m\left(\mathscr{P}(U_{I_0}, \cdots, U_{I_{n'-1}})\right)$$

$$= \left(\frac{1}{2K}\right)^{n'-1} \sum_{q=0}^{n'-1} \left\{ \sum_{k=0}^{\lfloor U_{I_q + 1} \rfloor} (-1)^k C_n^k \right.$$

$$\times \frac{n(\beta - k)^{n+1} + k(n + 1)(\beta - k)^n}{(n + 1)!} - \sum_{k=0}^{\lfloor U_{I_q} \rfloor} (-1)^k$$

$$\left. \cdot C_n^k \frac{n(\beta - k)^{n+1} + k(n + 1)(\beta - k)^n}{(n + 1)!} \right\}. \quad (18)$$

This is used to calculate the average first moment of the selected subset of the parallelepipeds, $F_m(\mathscr{QTC}_{n'})$. The average energy per two dimensions of the N-domain is equal to

$$P_2(\mathscr{QA}_N^{N'}(K, T)) = \frac{2R_2^2}{N} \frac{(2K)^{n'}}{T} F_m(\mathscr{QTC}_{n'}). \quad (19)$$

It is easy to show that the volume of $\mathscr{QA}_N^{N'}$ is equal to

$$V(\mathscr{QA}_N^{N'}(K, T)) = (\pi R_2^2)^n \frac{T}{(2K)^{n'}}. \quad (20)$$

Equations (19) and (20) can be used to calculate the tradeoff.

From Fig. 3, it is seen that for $N' = N/2$ ($n' = 2$), the tradeoff curves for the $\mathscr{A}_N^{N'}$ regions lie very near to the optimum curves. This suggests selecting $N' = N/2$ for the $\mathscr{A}_N^{N'}$ and also for the $\mathscr{QA}_N^{N'}$ regions. Fig. 5 shows the tradeoff curves of the $\mathscr{QA}_N^{N/2}$ regions as a function of K [computed using (19) and (20)]. The cases of $K = \infty$ are computed using the same approach as used in the case of Fig. 3. It is seen that, in general, the suboptimality caused by applying a coarse quantization to $\mathscr{TC}_{n'}$ is negligible. This is an example of the following phenomenon.

Although the volume has, in general, an exponential growth with the dimensionality, the number of energy shells required by a later shaping stage to be effective remains quite low. This is the basis for the direct addressing decomposition scheme proposed in the companion paper [15]. In the following section, we explain an addressing scheme to achieve the points marked in Fig. 5.

For $\psi' = 1/2$, the region $\mathscr{TC}_{n'}$ is equal to the Voronoi region of the lattice $\mathscr{D}_{n'}^*$ in the positive coordinates. Unlike the case of the $\mathscr{A}_N$ regions, we cannot use this property to achieve a point on the corresponding tradeoff curves. This is due to the fact that in this case, the density of points within $\mathscr{TC}_{n'}$ is no longer constant. However, we can still use this property to achieve points very near to these curves. To do this, the equal volume partitions (energy shells) of $\mathscr{A}_{N'}$ are mapped to equally spaced points along a dimension. The Voronoi region of $D_2^* = \Re Z^2$ is used to select half the points in the corresponding Cartesian product. This results in $r_s = 3$ ($CER_s = (8)^{2/N}$). The
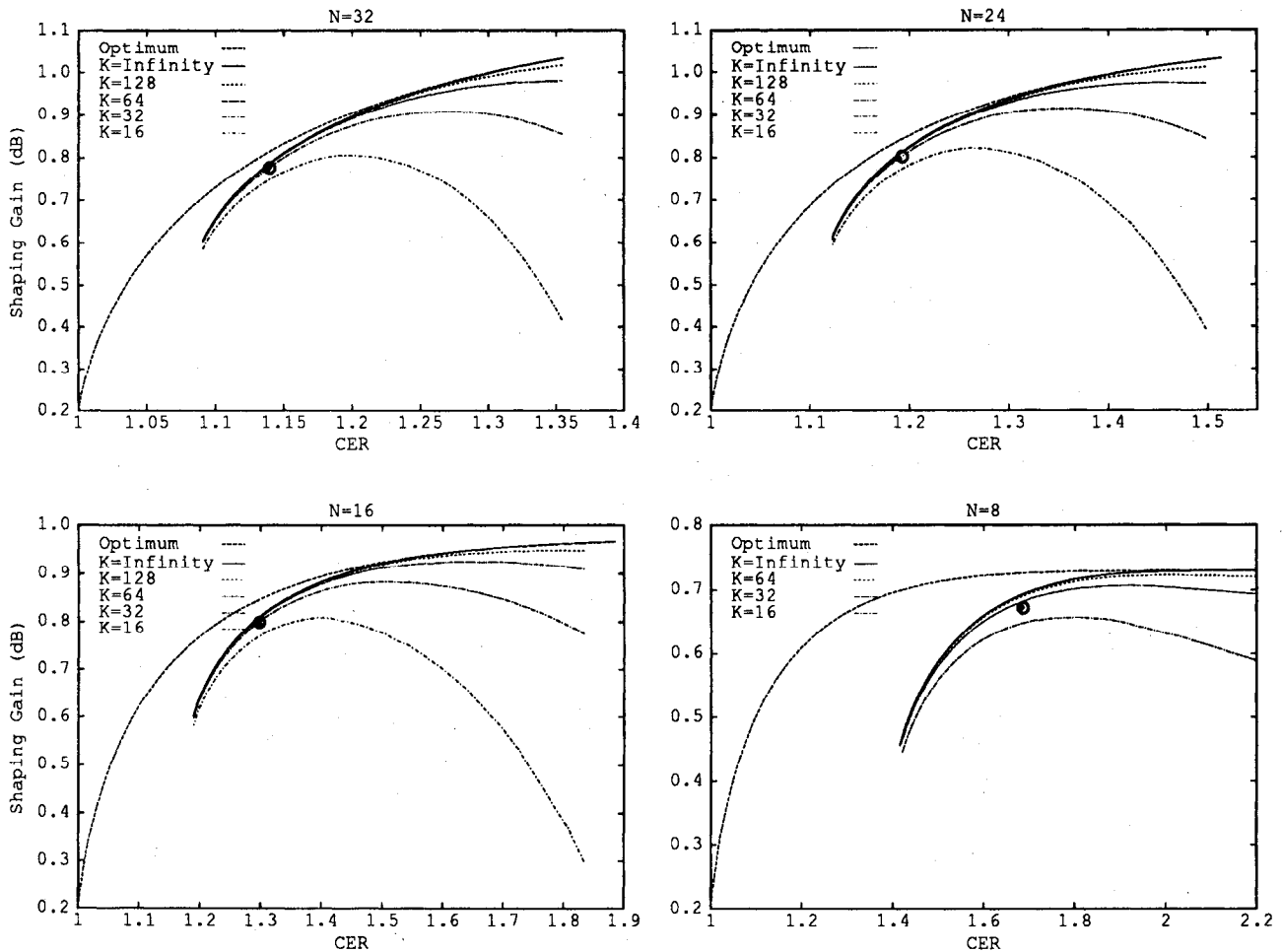
Fig. 5. Tradeoff between CER_s and γ_s in $\mathscr{BA}_N^{N'}(K,T)$ regions, $N = 8, 16, 24, 32$, $N' = N/2$.

point marked in Fig. 5 corresponds to such a region for $K = 128$. It is seen that the degradation is small. The B-points in Fig. 2 and Table I are optimum tradeoff points with the same value of CER_s.

VII. SUMMARY AND CONCLUSIONS

The structure of the regions which provide the optimum tradeoff between γ_s and CER_s and between γ_s and PAR in a finite dimensional space is introduced. Analytical expressions are derived for the corresponding tradeoff curves. In general, the initial parts of the curves have a steep slope. This means that an appreciable portion of the maximum shaping gain, corresponding to a spherical region, can be achieved with a small value of CER_s, PAR. The technique of shell mapping is introduced. This is a change of variable which maps the optimum shaping region to a hypercube truncated within a simplex. This mapping is a useful tool in computing the performance, and also in facilitating the addressing of the optimum shaping region. Using the shell mapping, a practical addressing scheme is presented that achieves a point on the optimum tradeoff curves. For dimensionalities around 12, the point achieved is located near the knee of the corre-

sponding tradeoff curve. For larger dimensionalities, a shaping region with two degrees of freedom is used. This region provides more flexibility in selecting the tradeoff point.

A. Recent Related Work

After revising this paper, we became aware that Laroia in [17] and Kschischang and Pasupathy in [18] (also refer to Kschischang [19]) have arrived at a similar shaping region as the one presented here. References [18] and [19] also give expressions for the optimum tradeoff curves (finite dimensional) using a different approach from ours. The same references nicely formulate and apply the addressing scheme of Lang and Longstaff [6] to an optimally shaped constellation.

Laroia, et al in [20] (also refer to [17]) apply ideas developed by the first two authors in the context of a type of structured vector quantizer to constellation addressing. This results in an addressing scheme which is similar to the scheme of [6]. They also suggest methods based on aggregating the energy shells to reduce the computational complexity. A comparison between their method and ours is provided in [15].

Kschischang in [21] discusses the structure of a prefix code which closely approximates the optimum nonuniform probabilities of the 2-D points.

More recently, a variant of the shell mapping technique is suggested by the Motorola Information Systems Group for inclusion in the forthcoming V.fast modem standard [22].

APPENDIX
INTEGRAL OF $F(X_0^2 + \cdots + X_{N-1}^2)$ OVER THE $\mathscr{A}_N$ REGION

We calculate the integral of the function $F(X_0^2 + \cdots + X_{N-1}^2)$ over the region $\mathscr{A}_N$ (N even) defined by (5). The calculation is based on decomposing the region $\mathscr{TC}_n$, defined by (8), into the union and intersection of the simplexes and applying Dirichlet's integral [16] to each of them. An example of this decomposition for $N = 4$ ($n = 2$) is shown in Fig. 6.

Applying the change of variable in (7), we obtain

$$I = \int_{\mathscr{A}_N} F(X_0^2 + \cdots + X_{N-1}^2) \, dX_0 \cdots dX_{N-1}$$

$$= (\pi R_2^2)^n \int_{\mathscr{TC}_n} F[R_2^2(Y_0 + \cdots + Y_{n-1})] \, dY_0 \cdots dY_{n-1}. \tag{21}$$

Define the n-D regions

$$\mathscr{C}_n = \{Y_p, \, p = 0, \cdots, n-1\}$$
$$: 0 \le Y_p \le 1, \tag{22}$$

$$\mathscr{T}_n(\alpha_0, \alpha_1, \cdots, \alpha_{n-1}; \beta)$$
$$= \{Y_p, \, p = 0, \cdots, n-1\}$$
$$: \alpha_0 \le Y_0 \le B + \alpha_0,$$
$$\alpha_1 \le Y_1 \le B + \alpha_1 - Y_0,$$
$$\cdots$$
$$\alpha_{n-1} \le Y_{n-1}$$
$$\le B + \alpha_{n-1} - Y_0 - \cdots - Y_{n-2};$$
$$\text{where } B = \beta - \sum_i \alpha_i, \tag{23}$$

and

$$\mathscr{Q}_n(\alpha_0, \alpha_1, \cdots, \alpha_{n-1}) = \{Y_p, \, p = 0, \cdots, n-1\}$$
$$: Y_p \ge \alpha_p. \tag{24}$$

Using this notation, the $\mathscr{TC}_n$ region can be written as

$$\mathscr{TC}_n = \mathscr{T}_n((0)^n; \beta) \cap \mathscr{C}_n. \tag{25}$$

We also define

$$\mathscr{Q}_n[(0)^{n-k}, (1)^k] = \sum \mathscr{Q}_n(i_0, \cdots, i_{n-1}) \tag{26}$$

where $i_0, \cdots, i_{n-1}$ is an n-tuple with k ones and $n - k$ zeros and the summation is calculated over all the C_n^k possible combinations of this type. Using these definitions, we can write

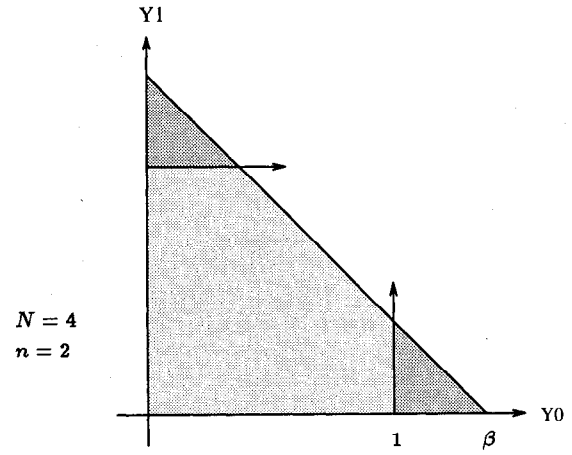$$\mathscr{C}_n = \sum_{k=0}^{n} (-1)^k \mathscr{Q}_n[(0)^{n-k}, (1)^k]. \tag{27}$$

Fig. 6. Example of decomposing into simplexes, $\mathscr{TC}_2 \, (1, \beta) = \mathscr{T}_2 (0, 0; \beta) - \mathscr{T}_2 (0, 1; \beta) - \mathscr{T}_2 (1, 0; \beta)$.

Using (27) in (25), we obtain

$$\mathscr{TC}_n = \sum_{k=0}^{n} (-1)^k \{ \mathscr{T}_n((0)^n; \beta) \cap \mathscr{Q}_n[(0)^{n-k}, (1)^k] \}. \tag{28}$$

It is easy to verify that

$$\mathscr{T}_n((0)^n; \beta) \cap \mathscr{Q}_n[(0)^{n-k}, (1)^k] = \varnothing, \quad \text{for } k \ge \lfloor \beta \rfloor + 1$$

where $\lfloor \beta \rfloor$ denotes the largest integer smaller than β. Combining (26) and (28) and using

$$\mathscr{T}_n((0)^n; \beta) \cap \mathscr{Q}_n(i_0, \cdots, i_{n-1}) = \mathscr{T}_n(i_0, \cdots, i_{n-1}; \beta), \tag{29}$$

we obtain

$$\mathscr{TC}_n = \sum_{k=0}^{\lfloor \beta \rfloor} (-1)^k \sum \mathscr{T}_n(i_0, \cdots, i_{n-1}; \beta) \tag{30}$$

where the second summation is calculated over all the combinations of $(i_0, \cdots, i_{n-1})$ with k ones and $n - k$ zeros. An example of this summation is shown in Fig. 6.

The integrand in (21) is symmetric with respect to the variables, and any permutation of the variables does not change its value. Consequently, the integral over the region $\mathscr{T}_n(i_0, \cdots, i_{n-1}; \beta)$ is independent of the permutation applied to $i_0, \cdots, i_{n-1}$. We calculate this integral over one of these regions, say over $\mathscr{P}_n(k, \beta) = \mathscr{T}_n((1)^k, (0)^{n-k}; \beta)$, and multiply the result by C_n^k. This results in

$$I = (\pi R_2^2)^n \sum_{k=0}^{\lfloor \beta \rfloor} (-1)^k C_n^k$$

$$\cdot \int_{\mathscr{P}_n(k, \beta)} F[R_2^2(Y_0 + \cdots + Y_{n-1})] \, dY_0 \cdots dY_{n-1}. \tag{31}$$

The integral over the region $P_n(k, \beta)$ in (31) can be written as

$$\int_{\mathscr{P}_n(k, \beta)} F\left[R_2^2(Y_0 + \cdots + Y_{n-1})\right] dY_0 \cdots dY_{n-1}$$

$$= \int_0^{\beta-k} \int_0^{\beta-k-Y_0} \cdots \int_0^{\beta-k-Y_0 - \cdots - Y_{n-2}}$$

$$\cdot F\left[R_2^2(Y_0 + \cdots + Y_{n-1} + k)\right] dY_0 \cdots dY_{n-1}. \quad (32)$$

The region of integration in (32) is a simplex of edge length $\beta - k$. Applying Dirichlet's integral [16] to this simplex results in (9) of the main text.

References

[1] A. R. Calderbank and L. H. Ozarow, "Nonequiprobable signaling on the Gaussian channel," *IEEE Trans. Inform. Theory*, vol. 36, pp. 726–740, July 1990.

[2] L. F. Wei, "Trellis coded modulation with multidimensional constellations," *IEEE Trans. Inform. Theory*, vol. 33, pp. 483–501, July 1987.

[3] G. D. Forney and L.-F. Wei, "Multidimensional constellations— Part I: Introduction, figures of merit, and generalized cross constellations," *IEEE J. Select. Areas Commun.*, vol. 7, pp. 877–892, Aug. 1989.

[4] J. H. Conway and N. J. A. Sloane, "A fast encoding method for lattice codes and quantizers," *IEEE Trans. Inform. Theory*, vol. 29, pp. 820–824, Nov. 1983.

[5] G. D. Forney, "Multidimensional constellations—Part II: Voronoi constellations," *IEEE J. Select. Areas Commun.*, vol. 7, pp. 941–958, Aug. 1989.

[6] G. R. Lang and F. M. Longstaff, "A leech lattice modem," *IEEE J. Select. Areas Commun.*, vol. 7, pp. 968–973, Aug. 1989.

[7] T. R. Fischer, "A pyramid vector quantizer," *IEEE Trans. Inform. Theory*, vol. 32, pp. 568–583, July 1986.

[8] G. D. Forney, "Trellis shaping," *IEEE Trans. Inform. Theory*, vol. 38, pp. 281–300, Mar. 1992.

[9] F. R. Kschischang and S. Pasupathy, "Optimal nonuniform signaling for Gaussian channels," *IEEE Trans. Inform. Theory*, vol. 39, pp. 913–929, May 1993.

[10] J. R. Livingston, "Shaping using variable-size regions," *IEEE Trans. Inform. Theory*, vol. 38, pp. 1347–1353, July 1992.

[11] A. R. Calderbank and M. Klimesh, "Balanced codes and nonequiprobable signaling," *IEEE Trans. Inform. Theory*, vol. 38, pp. 1119–1122, May 1992.

[12] A. K. Khandani, "Shaping multi-dimensional signal spaces," Ph.D. dissertation, McGill Univ., Mar. 1992.

[13] J. H. Conway and N. J. A. Sloane, *Sphere Packings, Lattices and Groups.* New York: Springer-Verlag, 1988.

[14] A. K. Khandani and P. Kabal, "An efficient addressing scheme for the nearly optimum shaping of multi-dimensional signal spaces," submitted to *IEEE Trans. Inform. Theory*, Aug. 1992.

[15] ——, "Shaping multidimensional signal spaces—Part II: Shell-addressed constellations," *IEEE Trans. Inform. Theory*, this issue, pp. 1809–1819.

[16] E. T. Whittaker and G. N. Watson, *A Course of Modern Analysis*, 4th ed. Cambridge, England: Cambridge Univ. Press, 1963.

[17] R. Laroia, "On optimal shaping of multidimensional constellations —An alternative approach to lattice-bounded (Voronoi) constellations," submitted to *IEEE Trans. Inform. Theory*, Nov. 1991.

[18] F. R. Kschischang and S. Pasupathy, "Optimal shaping properties of the truncated polydisc," submitted to *IEEE Trans. Inform. Theory*, 1992.

[19] F. R. Kschischang, "Shaping and coding gain criteria in signal constellation design," Ph.D. dissertation, Univ. Toronto, June 1991.

[20] R. Laroia, N. Farvardin, and S. Tretter, "On SVQ shaping of multidimensional constellations—High-rate large-dimensional constellations," in *Proc. 26th Annu. Conf. Inform. Sci. Syst.*, Princeton, NJ, Mar. 1992, pp. 527–531.

[21] F. R. Kschischang, "Huffman codes for shaping gain," in *Proc. 16th Biennial Symp. Commun.*, Kingston, Ont., May 1992, pp. 79–82.

[22] Motorola Information Systems Group, "Signal mapping and shaping for V. fast." Contribution D196, CCITT Study Group XVII, June 1992.